From scaffold to structure: the synthetic production of cell derived extracellular matrix for liver tissue engineering

Biomedical Physics & Engineering Express

ENDORSED BY IPEM Institute of Physics and Engineering in Medicine

ACCEPTED MANUSCRIPT • OPEN ACCESS

From scaffold to structure: the synthetic production of cell derived extracellular matrix for liver tissue engineering

To cite this article before publication: Rhiannon Grant *et al* 2018 *Biomed. Phys. Eng. Express* in press https://doi.org/10.1088/2057-1976/aacbe1

From scaffold to structure: the synthetic production of cell derived extracellular matrix for liver tissue engineering

Rhiannon Grant MSc, David Hay PhD, Anthony Callanan PhD

Institute for Bioengineering, School of Engineering, University of Edinburgh, King's Buildings, Mayfield Road, Edinburgh, EH9 3JL

Corresponding author; anthony.callanan@ed.ac.uk

Rhiannon Grant MSc

Email	rhiannon.grant@ed.ac.uk
Telephone	+44 (0)1316517077
Fax	+44 (0)131 650 6554

David C Hay PhD

Email	davehay@talktalk.net
Telephone	+44 (0)1316519500
Fax	+44 (0)131 651 9501

Anthony Callanan PhD

Email	anthony.callanan@ed.ac.uk
Telephone	+44 (0)1316507355
Fax	+44 (0)131 650 6554

Abstract

Liver transplant is the only curative treatment option for patients with end-stage liver failure, however there are few donor livers available for transplant. Tissue engineering of a human liver would potentially solve the problem of escalating donor shortages. A major challenge presents itself in the form of the hepatic extracellular matrix (ECM); a finely controlled *in vivo* niche which supports hepatocytes and plays a critical role in the development of liver disease. Polymers and decellularized tissues each provide some of the necessary biological cues for the hepatocytes, however, neither alone has proved sufficient. Equally, the ability to fine tune the microenvironment using bioactive molecules presents researchers with the opportunity to create personalised niches for hepatocytes, representing both normal and diseased phenotypes. This study combines cell derived ECM with a fibronectin vector and electrospun scaffolding techniques to produce a platform for creating customisable ECM microenvironments for hepatocytes (Abstract image). The resulting poly-L-lactic acid-extracellular matrix (PLA-ECM) scaffolds were validated using HepG2 hepatocytes.

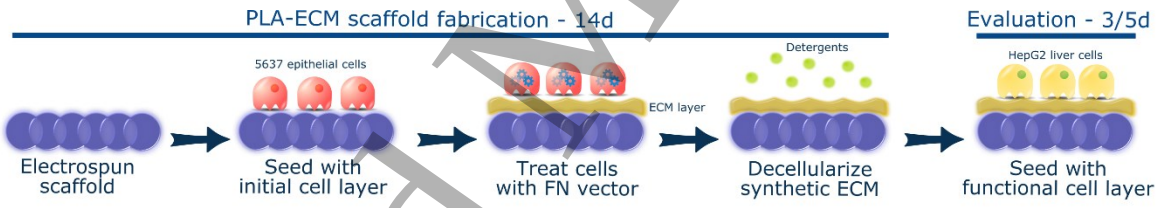

Abstract image. Methodology used to biofuctionalize electrospun scaffolds with synthetically derived ECM.

As expected, statistically significant mechanical differences were observed between the synthetically derived ECM (SD-ECM) scaffolds and normal ECM (N-ECM) scaffolds, confirming that the ECM has been altered by the fibronectin producing vector. The PLA-ECM scaffolds maintained hepatocyte growth and function and influence the gene expression of key hepatic genes. Furthermore, immunohistochemistry showed SD and N-ECMs differed in ratios of Collagen I, Laminin and Fibronectin.

Our results demonstrate that hybrid PLA-ECM scaffolds and the synthetic production of ECM provide a viable, translatable platform for customising microenvironments for hepatocytes.

This technology offers a potential solution to current obstacles in regenerative medicine, disease modelling and whole organ tissue engineering.

Introduction

In the US alone, as of August 20th 2017, the Organ Procurement and Transplantation Network (OPTN) estimates 14,158 patients are waiting for a donor liver. With a lack of viable new pharmaceuticals, liver transplant remains the sole treatment option for end-stage disease patients [1]. Liver disease is an increasing burden on the health of the Western world, with both incidence and mortality increasing rapidly since 1970 [2]. Demand for donor livers far outstrips supply, and the incidence of liver disease shows no signs of slowing down [3].

Tissue engineers seek to solve this problem by engineering liver 'organoids'; laboratory created organs which can function as a liver in vivo [4–7]. The 3D environment exerts extensive influence on the behaviour and function of hepatocytes [6,8]. With this in mind, tissue engineers employ scaffold manufacturing technologies to create structures which encompass key characteristics of the native 3D ECM [9–14]. Several different methods of creating a scaffold are in use, and they can be made from a myriad of substances; both natural and synthetic [15], and enhanced with bio-decoration methods [8]. There has been particular focus on decellularization, which provides an ECM bioscaffold with the 3D site-specific vasculature required for hepatocyte function upon their repopulation of the organ [16]. Decellularized organs have been repopulated with hepatocytes and endothelial cells which subsequently survive and exhibit some level of function, clearly demonstrating the importance of the ECM in supporting hepatocyte survival and phenotype [17–21]. However, decellularization requires a human or animal source of whole, undamaged organs and while research is showing great promise, the field is fragmented and to date no scaffold has been created which allows hepatocytes to function as well as in vivo [22,23].

Synthetic biology and genetic engineering are vital tools for tissue engineers and have been used to alter gene expression, enhance intracellular imaging and study fundamental processes in hepatocytes [24–26]. Recently, synthetic biology tools have been successfully employed to direct both stem cell lineage and fate in 3D constructs [27,28], in the manipulation of biofilms for cell culture [29] and in the production of therapeutic proteins in *in vivo* systems [30,31]

demonstrating the ability of synthetic biology techniques to manipulate 3D environments and thus their potential benefit to the field of tissue engineering. Groundbreaking CRISPR [32–34] and minicircle vector [35–37] technologies have made the idea of therapeutic gene editing in humans a viable reality, however concerns exist regarding the safety and subsequently, the translatability of such tools with regards to patient treatment. Heavily publicised and tragic events such as the 1999 death of 18 year old Jesse Gelsinger [38] and the 2002 clinical trial in which four children developed leukaemia following gene therapy for their Severe Combined Immune Deficiency disease [39] have led to obvious worries regarding the safety of gene therapies. The inflammatory and immune modulating effects of damage-associated molecular patterns (DAMPs) such as foreign DNA fragments [40] are well documented, however clinical use of decellularized ECM in exogenic and allogenic form has demonstrated great promise, giving no immune response and showing regenerative potential. This paves the way for using synthetic biology to tissue engineer the ideal ECM environment. The ideal ECM would utilise synthetic biology and genetic technologies to their utmost, considerable, potential but remove any risk from the tools used; such as the genetically modified cells themselves.

Table 1; Advantages of a combinatorial approach to tissue engineering of liver environments.

	Polymer scaffolds		**Decellularized tissues**		**Vector technology**		**Combinatorial approach**
✓	Reproducible	✓	Provides biochemical cues of ECM	✓	Customizable protein profile	✓	Mechanically & proteomically customizable
✓	Mechanically customizable	✓	Vasculature exists within tissue	✓	Rapid production of desired proteins	✓	Cell lines used - donors avoided
✘	Does not provide complex biochemical cues of ECM	✘	Limited donors & donor safety	✘	Vector safety concerns	✓	Vectors removed - safety concerns abated

With the potential of synthetic biology for manipulation of protein production in mind, we set out to address this problem; developing a novel bio-active hybrid scaffold which possesses the potential for customizatioon of the ECM microenvironment. To date, no bioengineers have combined the promising fields of scaffold manufacture, decellularized tissue and synthetic biology. Here we report the first use of a sacrificial, transfected cell line to bio-functionalise an electrospun polymer scaffold for liver tissue engineering. We have successfully decellularized the bio-functionalised scaffold, and validated the platform using cells representative of the liver, HepG2s.

Materials and Methods

Electrospinning

A 10% wt/vol solution of poly-L-lactic acid (Goodman) and hexafluoroisopropanol (Manchester Organics) was dissolved overnight at room temperature with agitation. Solutions were placed into a 10ml syringe and pumped using syringe pump EP-H11 (Harvard Apparatus) into the EC-DIG electrospinning system (IME technologies) via a 27G bore needle under the following parameters;

Table 2; Electrospinning parameters

Volume per hour	Total volume	Mandrel:needle distance	Positive charge	Negative charge	Mandrel rotation	Needle movement
0.5ml	10ml	14 cm	16kV	-3kV	250rpm	100mm/s

The mandrel was coated in non-stick aluminium foil for collecting the electrospun fibres. The sheets of electrospun fibres were allowed to dry overnight in a fume hood when the electrospinning session was completed. The average fibre size was 1.48μm as calculated by ImageJ plugin 'DiameterJ' [41].

Scaffold Preparation

10mm discs of scaffold were cut from the dry fibre sheet. The scaffolds were soaked in 70% isopropyl alcohol for 10 minutes, rinsed three times in phosphate buffered saline for 15

minutes each and allowed to dry completely at room temperature. Scaffolds were placed into an antibiotic/antimycotic treatment solution of Dulbeccos Minimal Essential Media supplemented with 100U/ml penicillin, 100µg/ml streptomycin, 0.25µg/ml Fungizone® (amphotericin B) Anti-Anti solution (Gibco) for 1 hour.

Initial Layer Cell Seeding and Culture

Scaffolds were removed from the antibiotic/antimycotic treatment solution and rinsed three times for 15 minutes each in complete media; Dulbeccos Minimal Essential Media supplemented with 10% foetal bovine serum, 2mM L-glutamine, 100U/ml penicillin and 100µg/ml streptomycin (Gibco). They were then placed into a fresh 48 well tissue culture plate.

5637 human urinary bladder epithelials (ATCC) were cultured and expanded as per supplier recommendations, using the media described above. Cells for scaffold seeding were trypsinized using 0.25% Trypsin-EDTA (Gibco) from tissue culture flasks and counted using the trypan blue exclusion method. 1 x 10^5 cells at passage 23 were suspended in 100µl of complete media and seeded directly on to the scaffolds. The cells were allowed to incubate in this small volume on the scaffolds for 2 hours, before an additional 400µl of complete media was added.

Media was changed after 24 hours using standard methods and subsequently changed every 48 hours. Controls were scaffold only, i.e. not seeded with an initial cell layer and a 'normal' initial layer i.e. untransfected cells. Initial layers of cells were cultured for 7 days at 37ºC and 5% CO_2 in a humidified incubator.

Fibronectin Vector

Vectors were obtained from the DNASU plasmid repository. In brief, the human fibronectin gene (FN1) was placed into a retroviral expression vector, PJ1520. The insert sequence was verified by sequence analysis and restriction enzyme digest by DNASU. The vector was obtained in DH5-alpha T1 phage resistance *Escheria coli* glycerol stock. We cultured the E. coli under selective conditions; 100µg/ml ampicillin, 34µg/ml chloramphenicol and 7%wt/vol

sucrose in LB media. Plasmid extractions were performed using Cambridge Bioscience's Zyppy™ plasmid extraction kit following manufacturer's methods.

Transfections

Transfections were performed using Invitrogen Lipofectamine 3000®. Following titration experiments, a concentration of 1µg plasmid DNA and 0.75µL lipofectamine reagent per scaffold was chosen. The initial layer of 5637 epithelials was cultured on the scaffolds under standard conditions for 7 days. Transfection was performed on the 7th day. Scaffold-cell constructs were then placed into selective media containing 150µg/ml puromycin. The cell-scaffold constructs were cultured under selection for a further 7 days to allow production of the vector derived fibronectin before being decellularized.

Decellularization

Decellularization was performed under sterile conditions at room temperature (19 - 22ºC) and with agitation. Scaffolds were placed into 50ml falcon tubes and placed on a rotator at 20RPM. Scaffolds were washed with phosphate buffered saline (PBS) for 15 minutes and then rinsed in 10mM tris buffered saline (TBS) for 15 minutes.

The scaffolds were submerged in a 0.1% vol/vol Triton X-100 (Sigma-Aldrich) 1.5M potassium chloride (Acros Organics) 50mM TBS for 4 hours. They were rinsed for 15 minutes in 10mM TBS before being submerged in fresh 10mM TBS overnight.

Scaffolds were given a final rinse in 10mM TBS for 15 minutes before being incubated in complete media for 15 minutes and then transferred to new 48 well plates for seeding.

Functional layer Cell Seeding and Culture

HepG2 cells were trypsinized using standard methods from tissue culture flasks and counted using the trypan blue exclusion method. 1 x 10^5 cells at passage 17 were suspended in 100µl of complete media and seeded directly on to the scaffolds. The cells were allowed to incubate

in this small volume on the scaffolds for 2 hours, before an additional 400µl of complete media was added.

Media was changed after 24 hours and changed every 48 hours after the initial 24 hour adherence and recovery period. This functional layer (FL) of cells was cultured using standard methods for either 3 or 5 days at 37ºC and 5% CO_2 in a humidified incubator.

Live/Dead® Viability/Cytotoxicity assay

To determine cellular viability, cell/scaffold constructs were incubated with 10µm calcein and 2µm ethidium ho-modimer-1 (Ethd-1) for 30 minutes as part of the two colour live/dead assay (Molecular Probes). Calcein is actively converted to calcein-AM in living cells, which then appear green when excited during fluorescence microscopy. Ethd-1 only accumulates in dead cells, which subsequently appear red. The method allows differentiation between dead and viable cells. The scaffolds were rinsed three times in $CaCl_2$/$MgCl_2$ free PBS to remove excess dye and placed onto a standard microscope slide with a 25mm glass coverslip (VWR). All images were captured using a Zeiss Axio Imager fluorescent microscope (COIL, University of Edinburgh) at 40x magnification and post processed using ImageJ.

CellTiter-Blue® Cell viability assay

The assay was performed according to manufacturer's instruction (Promega). For each condition group, n = 5. Importantly, cell/scaffolds constructs were moved into fresh 48 well plates to prevent reading activity from tissue culture plastic bound cells. Measurements were read in a Modulus™ II microplate reader at an excitation wavelength of 525 nm and emission wavelength of 580-640 nm and reported as fluorescence.

Albumin quantification

A bromocresol green (BCG) albumin assay (Sigma) was used to quantify serum albumin produced by the HepG2 functional cell layer over 24 hours at 3 and 5 day timepoints. The

assay was performed according to manufacturer's instructions and results read at an absorbance of 620 nm in a Modulus™ II microplate reader.

Picogreen® DNA quantification

The Quant-IT™ Picogreen® dsDNA assay kit (Life Technologies™) was employed to establish the efficiency of the decellularization method in removing cellular material and to estimate cell number on the cell/scaffold constructs. The assay was performed according to manufacturer instructions. In brief, constructs (n = 5) were digested in a solution of $CaCl_2$ and $MgCl_2$ free PBS (Sigma), containing 2.5 U/ml papain extract (Sigma) 5 mM cysteine-HCl (Sigma) and 5 mM EDTA (Sigma) and incubated for 48 hours at 60°C. Picogreen solution was added to the digests and fluorescent intensity measurements read in a Modulus™ II microplate reader at an excitation wavelength of 480 nm and emission wavelength of 510-570 nm. A standard λ dsDNA curve of graded known concentrations was used to calibrate fluorescence intensity vs dsDNA concentration.

Sectioning and staining

The samples were rinsed three times in PBS (Gibco) for 15 minutes each, then fixed in 4% v/v formalin buffered in saline for 15 minutes at room temperature. After rinsing with fresh PBS, constructs were embedded in low melting temperature polyester wax (Electron Microscopy Supplies) using methods adapted from Steele et al. (2014). In brief, samples are dehydrated through 70-100% ethanol, then incubated in 50:50 ethanol:wax overnight at 45ºC overnight with agitation. The samples were moved into 100% wax for 3 hours at 45ºC and then fresh 100% wax for 1 hour at 45ºC. Samples were embedded and allowed 72 hours to fully cure before sectioning. Immunohistochemical staining was undertaken using antibodies for Collagen I (Stratech), Laminin (Stratech) and Fibronectin (Sigma). All images were captured using a Zeiss Axio Imager system (Centre Optical Instrumentation Laboratory, University of Edinburgh) at 40x magnification and post processed using ImageJ.

Scanning Electron Microscopy

SEM was used to characterise the scaffold architecture. Samples were rinsed three times in PBS for 15 minutes each, then fixed in 2.5% v/v glutaraldehyde (Fisher Scientific) in 0.1M phosphate buffer (PB) (pH 7.4) at 4ºC overnight. They were then rinsed three times in 0.1M PB before being post-fixed in 1% v/v osmium tetroxide (Electron Microscopy Supplies) buffered with 0.1M PB. Samples were again rinsed three times in 0.1M PB and dehydrated through an ethanol gradient (30-100%). They were dried by placing them in hexamethyldisilazane (HDMS, Sigma) which was allowed to evaporate off at room temperature overnight. We mounted the samples onto SEM chucks using double sided carbon tape and coated them with a thin layer of gold and palladium alloy (Polaron Sputtercoater).

All images were captured at 5 kV using a Hitach S-4700 SEM (BioSEM, University of Edinburgh).

Mechanical Testing

Nanoindentation experiments were undertaken to establish the dynamic properties of scaffolds and decellularized ECM/scaffold constructs using the Keysight/Agilent 5200 nano indenter testing system.

Scaffolds and constructs were subject to indentation by a DCM II actuator flat-ended cylindrical punch (D = 100μm) using a max load of 1g-f. All nanoindentation experiments were carried out on fresh, hydrated (suspended in PBS), unfixed samples in a stainless steel well chuck. A total of 36 indentations were carried out on each sample, 50nm apart. Indent sites were selected using the high precision X-Y stage within the testing system (Agilent). Poissons ratio was assumed to be 0.5 for each sample [42,43]. Allowable drift rate was 0.1nm/s. A NanoSuite (Keysight Technologies) test method “G-Series DCM CSM Flat Punch Complex Modulus” was used for all testing [44,45].

Gene Expression analysis

RNA was extracted from constructs using standard Trizol (Fisher Scientific) methods and purified using Qiagen's RNeasy spin column system. cDNA was synthesised using the Promega's ImProm-II™ Reverse Transcription System.

Quantitative real-time polymerase chain reaction (qRT-PCR) was performed using the LightCycler® 480 Instrument II (Roche Life Science) and Sensifast™ SYBR® High-ROX (Bioline) system. Results were normalized to HepG2s of the same passage number grown on tissue culture plastic and compared to the housekeeping gene Glyceraldehyde-3-Phosphate Dehydrogenase (GAPDH). Analysis was performed using the 2–[delta][delta] Ct method [46,47], n = 5. Albumin (Alb), Cytochrome P450 Family 1 Subfamily A Polypeptide 1 (Cyp1A1), Cytochrome P450 Family 1 Subfamily A Polypeptide 2 (Cyp1A2), Cytochrome P450 Family 3 Subfamily A Polypeptide 4 (Cyp3A4), Collagen Type I alpha 1 (Col1A1), Collagen Type 4 alpha 1 (Col4A1) and Fibronectin Type 1 (FN1) were investigated, forward and reverse primers (Sigma) are detailed in Supplementary Table 1.

Statistical Analysis

One-way ANOVAs with Fishers, Games-Howell and Tukey [48–50] post-hoc testing were performed using Minitab 17 Statistical Software and graphs generated using Origin software (OriginLab, Northampton, MA). Error bars indicate standard deviation. A minimum of n = 3 and max of n = 6 was used for all analysis.

Results

Cell attachment and survival on scaffolds

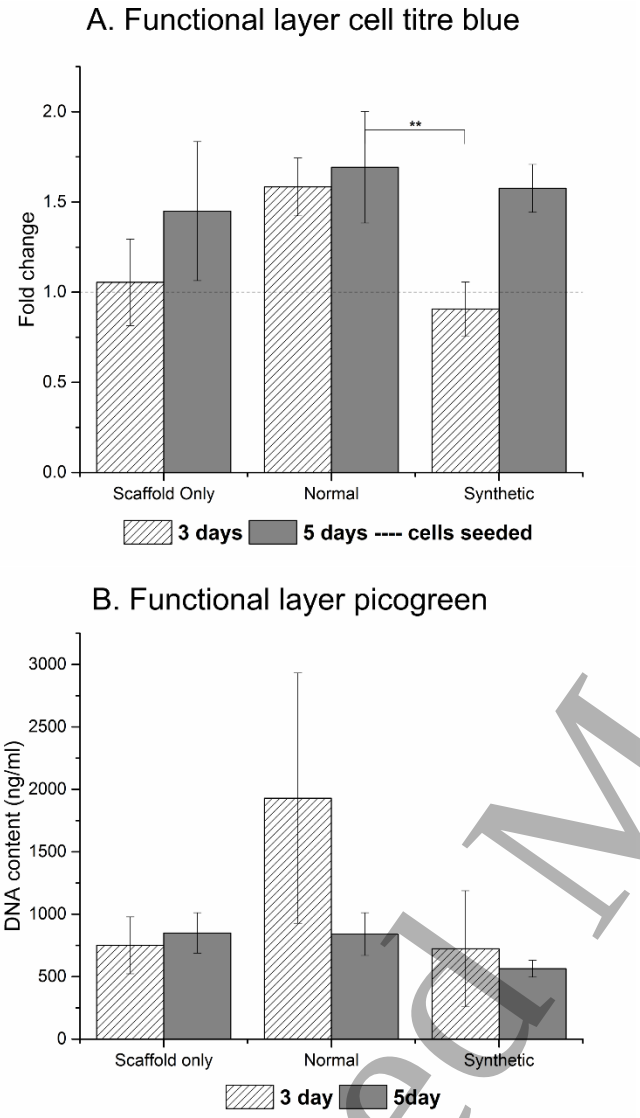

Figure 1. Cell titre blue assay indicating metabolic activity (A) and DNA quantitation of the functional layer (B). One way ANOVA with Games Howell post hoc testing, ** = p value <0.01.

When compared to normal ECM derived from untransfected cells (N-ECM) and the scaffold alone (SO), a lower number of HepG2s adhered to the synthetically derived vector driven (SD-ECM) scaffold-ECM constructs (Fig. 1). According to the CellTiter-Blue® results (Fig. 1A), the SD ECM layer maintained the growth of the HepG2s between days 3 and 5. However, this result is not concurrent with the Picogreen® DNA quantitation (Fig. 1B). This is most likely due to different data extraction methods and validation methods in the Picogreen and CellTiter-Blue assays. Both assays possess depth dependencies with regards to their efficiency and effectiveness in extracting data from fibrous scaffold constructs. Additionally, the assays were validated using 2D monolayer cell cultures. This would explain high standard deviations in the Picogreen® DNA quantitation dataset and slight different trends observed between the assays. These finding are corroborated by our recent published work of cells on electrospun scaffolds [14]. Live/Dead® Viability/Cytotoxicity images (Fig. 2) demonstrate the metabolic viability of the functional HepG2 cell layer (FL), and that at day 5 the cells appear to be confluent and living, with low levels of cell death in each condition.

Mechanical characterisation of scaffolds

Reassuringly, both storage (G') and loss (G") modulus demonstrate significant differences between the three conditions (Fig. 3). Fibronectin is known to influence both the mechanical profile of the ECM [51,52] and influence the maintenance and structure of other vital ECM proteins, such as collagen [53]. Equally, cells are known to respond to the mechanical and topographical influence a scaffold exerts [54].

Testing was performed at frequencies experienced by the human liver in vivo [55]. Storage modulus (G') ranged from 22.92±9.14 to 12.29±0.14 MPa and loss modulus (G") from 2.45±0.93 to 0.15±0.02 MPa at the frequencies detailed in supplementary tables 2 and 3.

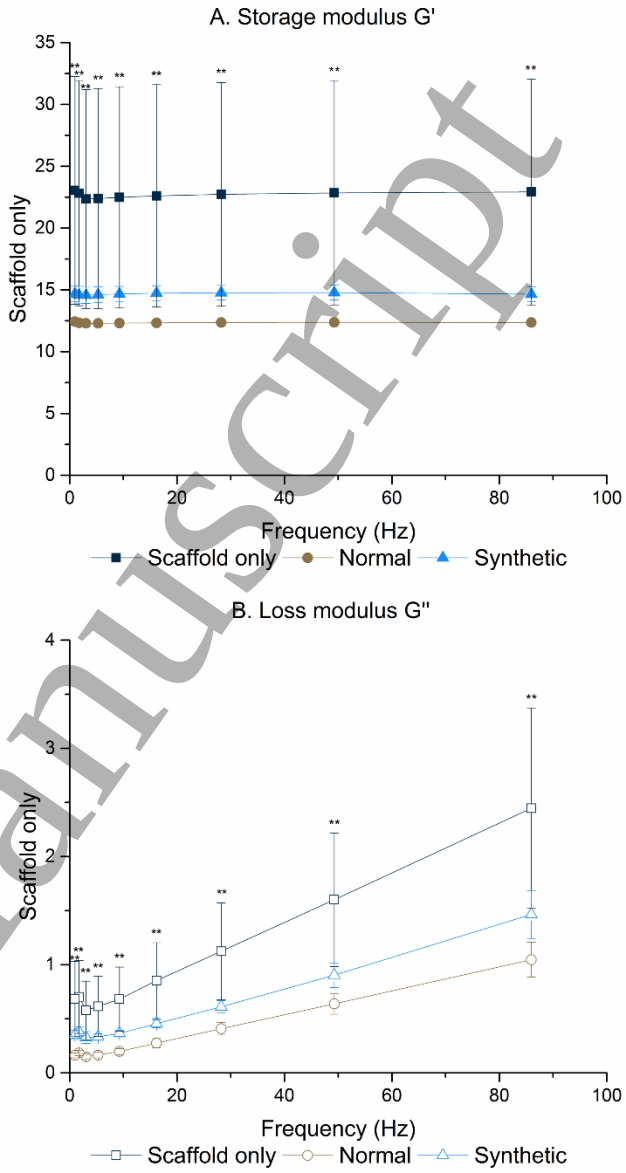

Figure 3. Significant mechanical differences were observed between all scaffold conditions. One way ANOVA with Games Howell post hoc testing, ** = p value <0.01.

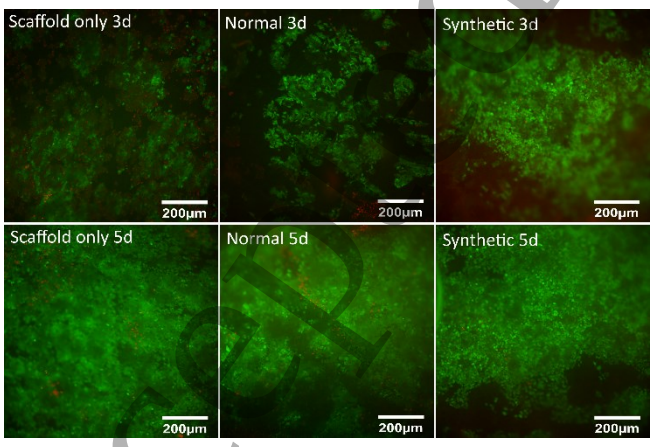

Figure 2. Live Dead imaging demonstrating the living functional layer present at each time point, with minimal cell death.

Biochemical characterisation of the hybrid polymer-ECM scaffolds

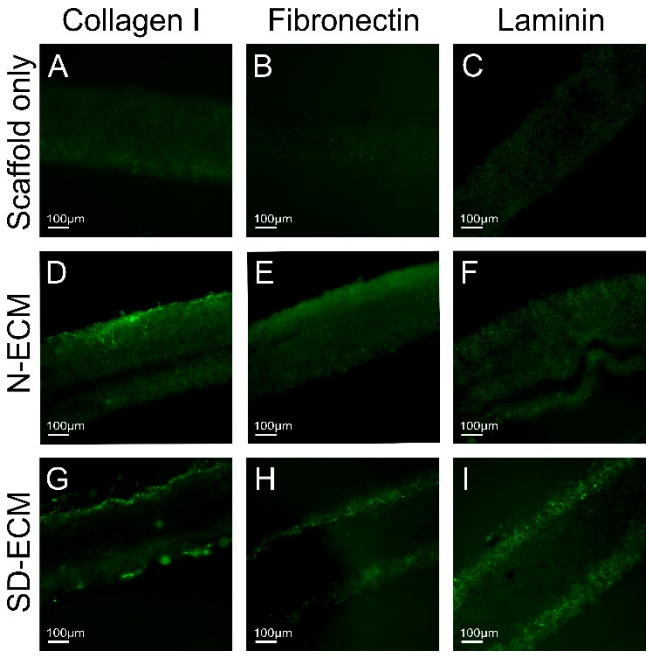

Figure 4. IHC staining showing the retention of major liver ECM proteins Collagen I (D, G), Fibronectin (E, H) and Laminin (F, I) following decellularization. Additionally, SO condition shows no positive staining as expected (A, B, C).

Differences in the biochemical profile of the different ECMs were demonstrated by immunohistochemistry performed on decellularized hybrid scaffold sections (Fig. 4). Hepatic cells are very responsive to extracellular matrix proteins; particularly Collagen I, Laminin and Fibronectin [56–58]. Fibronectin is ubiquitous in healthy liver [59,60], and antibody staining reveals altered levels of fibronectin in the synthetically derived ECM, as expected due to the introduction of the fibronectin vector (Fig. 4H). ECM proteins do not exist in isolation, and fibronectin is known to influence the generation and laydown of other ECM proteins including collagen I and laminin [53,61], as evidenced in Fig. 4G and 4I when compared to N-ECM. The N-ECM is collagen I rich (Fig. 4D) with some fibronectin and laminin also present (Fig. 4E & 4F). Of note is that the SD-ECM appears to be concentrated on the outer layers of the electrospun scaffold. This could be due to the transfected cells being in fewer number than those which were not transfected (N-ECM), so they did not penetrate the scaffold to the same extent.

Gene expression of HepG2s in response to hybrid polymer-ECM scaffolds

Genes associated with both liver function and ECM production were assayed for gene expression (Fig. 5). Albumin expression, a marker of appropriate liver cell differentiation and function, appears upregulated between day 3 and day 5 in each condition, confirming appropriate development of the cells. At day 5, expression is significantly upregulated in comparison to HepG2s grown on tissue culture plastic (TCP) on the SD-ECM constructs; with

the highest levels of expression observed in SO and SD-ECM conditions. Additionally, albumin mRNA expression is downregulated in comparison to TCP at day 3 in all conditions (Fig. 5A). Cytochrome P450s (Cyp) are a family of enzymes involved in metabolism of xenobiotics and toxic compounds in the liver [62–64]. Cyp1A1 mRNA expression is significantly altered in comparison to TCP (Fig. 5B); upregulated at day 3 and downregulated at day 5. Cyp1A2 mRNA expression is consistently significantly downregulated in all but one condition; day 3 N-ECM (Fig. 5C). Cyp3A4 mRNA expression is upregulated in every condition, with a significant upregulation observed in response to SD-ECM (Fig. 5D).

In addition, we assayed for three ECM genes important for normal liver composition [59,65]; Fibronectin (Fig. 5E), Collagen I (Fig. 5F) and Collagen IV (Fig. 5G). Considering the plastic nature of ECM, these genes are of interest with regards to ongoing modification of the tissue microenvironment despite hepatocytes not being the main producers of ECM proteins in the liver [59,66].

Collagen I is consistently upregulated, with significant upregulation observed at day 5 on SD-ECM. Equally, Fibronectin mRNA expression is significantly upregulated on day 5 SD-ECM constructs, though downregulated at day 3 on SO and N-ECM constructs. Collagen IV mRNA expression is consistently upregulated in each condition, with significant changes observed in all but day 3 N-ECM and SD-ECM. While such

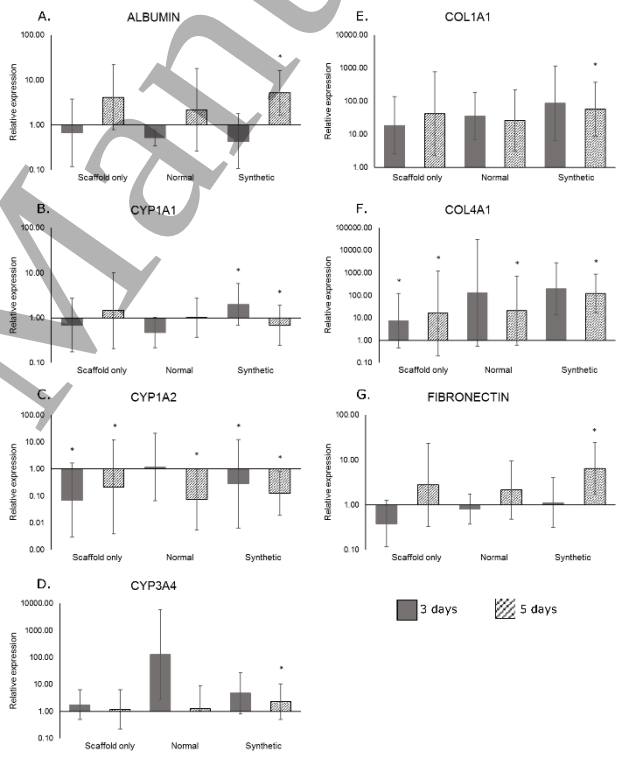

Figure 5. Q-PCR results showing significant changes in expression of major liver genes when compared to TCP, Albumin (A), CYP1A1 (B), CYP1A2 (C), CYP3A4 (D) an ECM genes Col 1A1 (E), Col 4A1 (F) and Fibronectin (G) between the hybrid scaffolds and tissue culture plastic. (A, C, D, E, F, G) = One way ANOVA with Games Howell post hoc testing, * = p value <0.05. (B) = One way ANOVA with Tukey post hoc testing, * = p value <0.05.

alterations in gene expression are promising, we refrain from further assumption regarding cell response without further proteomic and functional analyses.

Albumin production

Albumin levels are indicative of hepatocyte health and response to the microenvironment [57]. Each condition results in differing levels of albumin production, with significant differences in protein levels observed between SO and SD-ECM at both 3 days and 5 days (Fig. 6), indicating that the N-ECM encouraged albumin production more than SD-ECM.

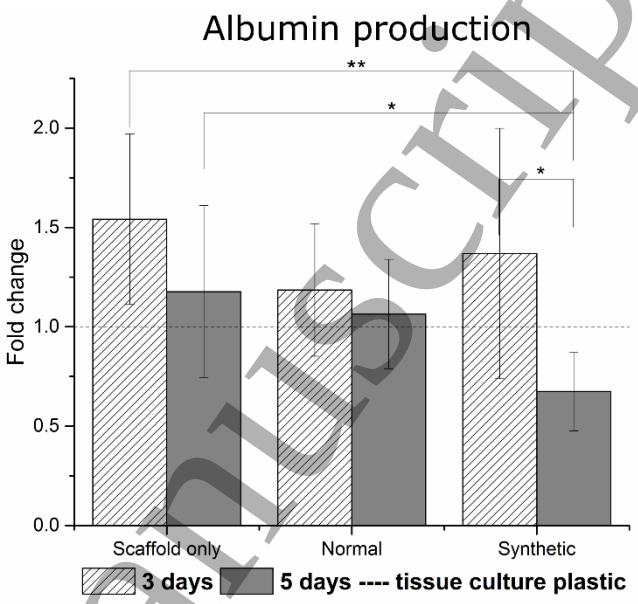

Figure 6. Albumin production between conditions, showing significant changes between SO and SD-ECM conditions at both time points. One way ANOVA with Games Howell post hoc testing, * = p value <0.05. ** = p value <0.01.

Confirmation of decellularization

Decellularization was confirmed using Picogreen® DNA quantitation (Fig. 7G) and histological staining (Fig. 7A-F). A tenfold reduction in DNA combined with visual confirmation of an absence of DAPI nuclear staining and Phalloidin-514 actin staining on

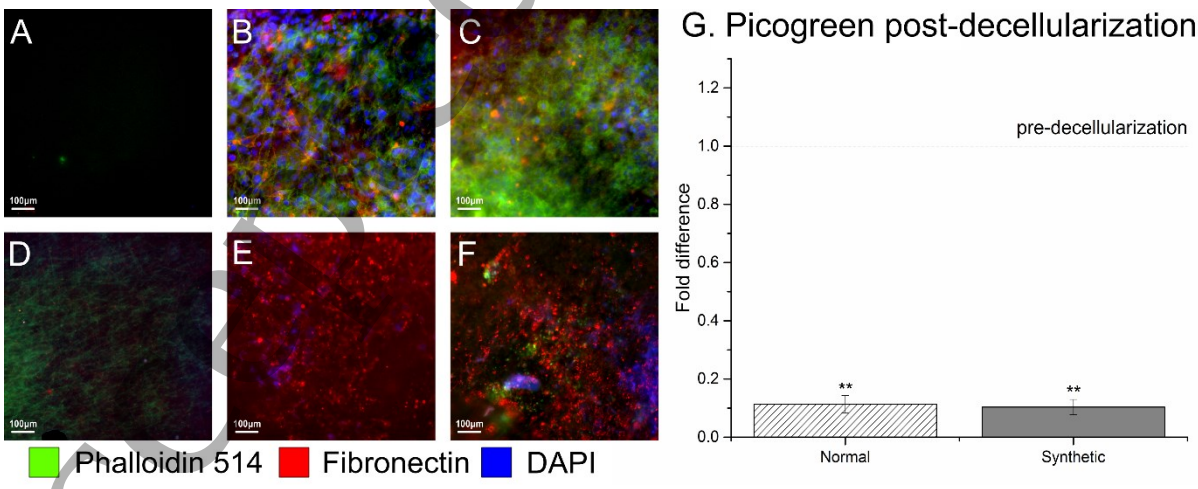

Figure 7. Effectively decellularized constructs, with minimum remnant DNA detected by IHC (E,F) or picogreen (G). Scaffolds pre-decellularization shown in (A), (B) and (C). One way ANOVA with Games Howell post hoc testing, ** = p value <0.05. Scaffold only (A, D), N-ECM (B,E) and SD-ECM (C, F)

decellularized constructs, plus the presence of fibronectin antibody staining on both the N-ECM and SD-ECM decellularized constructs (Fig. 7E&F) provides evidence of efficient decellularization methods, and that synthetically derived fibronectin is present on the hybrid scaffolds.

Discussion

The extracellular matrix provides a microenvironment for cells which is not yet fully understood, nor replicable by existing manufacturing methods [16,67–69]. By manipulating human cells to produce a customizable blend of ECM components, and combining this with replicable electrospun scaffolds and decellularization methods we overcome the shortage of donor derived ECM bioscaffolds and the issues regarding animal-sourced biomaterials [16,70]. Additionally, this platform has the potential to be used to model not only 'healthy' ECM microenvironments, but also those of disease and developing states.

By using fibrous electrospun scaffolds we mimic the morphology of healthy fibrillary collagen [10,11,71,72]. PLA was used to fabricate the scaffolds, chosen for its compatibility with hepatocytes [56] and its use in multiple types of medical device due to its predictable biodegradation rate and mechanical properties [73,74].

Fibronectin was chosen as our protein to synthetically overexpress due to its vital role in the liver [51,75] and its interaction with other ECM components such as collagen and laminin [52,53]. Fibronectin is a large dimeric adhesive glycoprotein which exists in both cellular and plasma forms, with roles in regenerating tissues, embryonic development and regulation of cell behaviours such as adhesion and migration [76]. The role of fibronectin in the liver is still unclear, with inhibition of fibronectin production or deposition improving fibrosis outcomes [77,78]. However its vital role in the hepatic ECM is demonstrated by mutant mice who were specifically null in only the liver for both plasma and cellular fibronectin. The fibronectin-null livers not only develop highly disorganized/diffuse collagenous ECM networks, but when fibrogenesis was induced the null livers experienced more extensive fibrosis; thought to be

due to fibronectins role in regulating TGF-β1 bioavailability [75]. Additionally, homozygous fibronectin null mutants display early embryonic lethality, while heterozygotes (with 50% of the normal plasma fibronectin levels) appear normal; suggesting a dose dependent role for fibronectin in development [79].

As an initial assessment of these novel hybrid scaffolds we investigated the attachment and function of a commonly used liver cell line, HepG2s, when cultured on the synthetically derived hybrid scaffolds versus a wild type 'normal' hybrid scaffold and the scaffold alone. The HepG2 cell line was derived from the hepatocarcinoma of a 15 year old Caucasian male. They are often used because they are virus free, possess liver specific functions such as ammonia metabolism and albumin synthesis and secrete some growth factors [80]. We analysed cell attachment and viability, albumin production and gene expression of both liver function genes and ECM genes at 3 and 5 day time points. Additionally, we validated our decellularization method and performed both immunohistochemical and raman spectrum analyses (data not shown) of the hybrid scaffold-ECM constructs upon which the HepG2s were seeded.

Our results indicate not only that synthetically derived ECMs provide a viable method of biofunctionalising electrospun polymer scaffolds, but that the composition of the synthetically derived ECM-polymer hybrid scaffolds influences liver cells. That albumin production is significantly altered between SO and SD-ECM conditions, but not N-ECM conditions supports this assertion. Gene expression of key hepatic genes was altered on day 5 of SD-ECM conditions in every gene tested, whereas SO and N-ECM conditions only influence CYP1A2 and COL4A1 expression; demonstrating that the composition of the ECM is highly influential in tissue engineering. This in turn leads to questions regarding donor-donor variability of current decellularization work and its influence upon hepatic behaviour and a need for more reproducible hepatic microenvironments that this platform provides.

The researchers responsible recognise that, while this study forms a robust initial proof of principle regarding the exploitation of synthetic biology for scaffold manufacture, and has produced a novel hybrid synthetically derived ECM- polymer scaffold with great potential for

liver tissue engineering, further work is required to analyse results and increase translatability. Vector technologies and synthetic biology present obvious concerns with regards to patient safety [30,81], and care should be taken to ensure all bacterial/ viral constructs are removed from the ECM layer. Detergent based methods used to strip the ECM of cells can be detrimental to the bioscaffold [70,82], disrupting native tissue ultrastructure, decreasing glycosaminoglycan (GAG) content and reducing collagen integrity [83,84] as well as disrupting lipid-lipid, lipid-protein and protein-protein interactions [85]. Care should be taken to optimise this procedure in the future. HepG2s provide a convenient method of initial viability testing of the scaffolds, but they are derived from a carcinoma and as such criticism of their clinical relevance is well placed. Further studies will utilise primary or stem cell derived hepatocytes to combat such criticism. Additionally, recognition of the value of further proteomic and functional assays (such as ELISAs and Alkaline Phosphatase quantitation) in analysing the function of hepatocytes will be vital for expanding this work, however at this time these were deemed unnecessary considering the obvious critiques of the use of the HepG2 cell line. Further, the importance of ensuring decellularization agents are removed from the constructs should not be underestimated, due to their influence upon cells and ECM [21,70]. While such criticisms are important to consider, this work clearly demonstrates the potential of synthetic biology for the design of bespoke ECMs and provides a robust initial platform upon which further, improved studies can be built.

Conclusion

This study demonstrates a novel method of creating a biologically bespoke hybrid ECM-polymer scaffold; utilising clinically translatable electrospun scaffold technologies and synthetic biology methods both easily modified to fulfil Good Manufacturing Practice (GMP) guidelines. In order to achieve this, a sacrificial ECM-producing cell layer was transfected using a protein producing fibronectin vector on an electrospun scaffold, biofuctionalizing the scaffold with a biologically bespoke ECM. Scaffolds with wild type untransfected cells and no initial cell layer at all were used as controls. This sacrificial cell layer was successfully removed

with a detergent based method and the hybrid synthetically derived ECM-polymer scaffolds seeded with HepG2 liver cells for validation. Results were validated using multiple well characterized methods, including mechanical quantitation, Q-PCR and immunohistochemistry. The synthetically derived PLA-ECM scaffolds exert biological influence upon liver cells, manipulating their microenvironment and resulting in alterations in gene expression profile, protein synthesis and cell attachment and survival. Such data demonstrates promise as a unique method of creating biologically bespoke ECMs and exerting influence upon cell populations both *in vivo* and *in vitro*.

These novel scaffolds exhibit great promise both as an implantable patient treatment for liver tissue engineering, for adaptation to other tissues and as a useful tool for development of 3D liver cell culture platforms with potential for both *in vivo* cell analysis and novel pharmaceutical research.

Acknowledgements

The authors would like to thank Prof Alistair Elfick for use of lab facilities (IBioE, University of Edinburgh). We would also like to thank Steve Mitchell (BioSEM) andDr David Kelly (COIL) (University of Edinburgh). This work is funded by an Engineering & Physical Sciences Research Council [EPSRC] doctoral training partnership studentship, UK Regenerative Medicine Platform II [RMPII] grant MR/L022974/1 and MRC computational and chemical biology of the stem cell niche grant (CCBN) MR/L012766/1.

Author disclosure

The authors declare no competing interests.

1. British Association for the Study of the Liver & British Society of Gastroenterology. A Time to Act: Improving Liver Health and Outcomes in Liver Disease. *Natl. Plan Liver Serv. UK* 1–52 (2009).
2. Williams, R. *et al.* Implementation of the Lancet Standing Commission on Liver Disease in the UK. *Lancet* **386,** 2098–2111 (2015).
3. Wang, H. *et al.* Global, regional, and national life expectancy, all-cause mortality, and cause-specific mortality for 249 causes of death, 1980–2015: a systematic analysis for the Global Burden of Disease Study 2015. *Lancet* **388,** 1459–1544 (2016).

4. Huch, M. *et al.* Long-term culture of genome-stable bipotent stem cells from adult human liver. *Cell* **160,** 299–312 (2015).

5. Ye, J., Shirakigawa, N. & Ijima, H. Hybrid organoids consisting of extracellular matrix gel particles and hepatocytes for transplantation. *J. Biosci. Bioeng.* (2015). doi:10.1016/j.jbiosc.2015.01.004

6. Takebe, T. *et al.* Vascularized and complex organ buds from diverse tissues via mesenchymal cell-driven condensation. *Cell Stem Cell* **16,** 556–565 (2015).

7. Banaeiyan, A. A. *et al.* Design and fabrication of a scalable liver-lobule-on-a-chip microphysiological platform. *Biofabrication* **9,** (2017).

8. Grant, R., Hay, D. & Callanan, A. A Drug-Induced Hybrid Electrospun Poly-Capro-Lactone: Cell-Derived Extracellular Matrix Scaffold for Liver Tissue Engineering. *Tissue Eng. Part A* **23,** 650–662 (2017).

9. Nichol, J. W. *et al.* Cell-laden microengineered gelatin methacrylate hydrogels. *Biomaterials* **31,** 5536–44 (2010).

10. McCullen, S. D., Autefage, H., Callanan, A., Gentleman, E. & Stevens, M. M. Anisotropic Fibrous Scaffolds for Articular Cartilage Regeneration. *Tissue Eng. Part A* **18,** 2073–2083 (2012).

11. Accardi, M. A. *et al.* Effects of fiber orientation on the frictional properties and damage of regenerative articular cartilage surfaces. *Tissue Eng. Part A* **19,** 2300–10 (2013).

12. Steele, J. A. M. *et al.* Combinatorial scaffold morphologies for zonal articular cartilage engineering. *Acta Biomater.* **10,** 2065–2075 (2014).

13. Noszczyk, B. H. *et al.* Biocompatibility of electrospun human albumin: a pilot study. *Biofabrication* **7,** 15011 (2015).

14. Grant, R., Hay, D. & Callanan, A. A drug induced hybrid electrospun PCL - cell derived ECM scaffold for liver tissue engineering. *Tissue Eng. Part A* ten.TEA.2016.0419 (2017). doi:10.1089/ten.TEA.2016.0419

15. Naderi, H., Matin, M. M. & Bahrami, A. R. Review paper: critical issues in tissue engineering: biomaterials, cell sources, angiogenesis, and drug delivery systems. *J. Biomater. Appl.* **26,** 383–417 (2011).

16. He, M. & Callanan, A. Comparison of methods for whole organ decellularisation in tissue engineering of bio-artificial organs. *Tissue Eng. Part B Rev.* **19,** (2012).

17. De Kock, J. *et al.* Simple and quick method for whole-liver decellularization: A novel in vitro three-dimensional bioengineering tool? *Arch. Toxicol.* **85,** 607–612 (2011).

18. Baptista, P. M. *et al.* The use of whole organ decellularization for the generation of a vascularized liver organoid. *Hepatology* **53,** 604–617 (2011).

19. Barakat, O. *et al.* Use of decellularized porcine liver for engineering humanized liver organ. *J. Surg. Res.* **173,** e11–e25 (2012).

20. Wu, Q. *et al.* Optimizing Perfusion-Decellularization Methods of Porcine Livers for Clinical-Scale Whole-Organ Bioengineering. *Biomed Res. Int.* **2015,** 1–9 (2015).

21. Zhou, P. *et al.* Decellularization and Recellularization of Rat Livers With Hepatocytes and Endothelial Progenitor Cells. *Artif. Organs* n/a-n/a (2016). doi:10.1111/aor.12645

22. Faulk, D. M., Wildemann, J. D. & Badylak, S. F. Decellularization and Cell Seeding of Whole Liver Biologic Scaffolds Composed of Extracellular Matrix. *J. Clin. Exp.*

Hepatol. **5,** 69–80 (2015).

23. Kogel, J. Van Der, Bussink, J., Coxon, A., Polverino, A. & M, P. Fluid flow regulation of revascularization and cellular organizationin a bioengineered liver platform. *Tissue Eng. Part C Methods* 1–22 (2016).
24. Hazama, K., Asayama, S. & Kawakami, H. Up-Regulation of Gene Expression by Transfection to Hepatocyte Spheroids. *Mol. Pharm.* (2012).
25. Lee, M. H. *et al.* Hepatocyte-Targeting Single Galactose-Appended Naphthalimide: A Tool for Intracellular Thiol Imaging in Vivo. *J. Am. Chem. Soc.* **134,** 1316–1322 (2012).
26. Lu, C., Xu, W., Zhang, F., Shao, J. & Zheng, S. Nrf2 Knockdown Disrupts the Protective Effect of Curcumin on Alcohol-Induced Hepatocyte Necroptosis. *Mol. Pharm.* **13,** 4043–4053 (2016).
27. Narsinh, K. H. *et al.* Generation of adult human induced pluripotent stem cells using nonviral minicircle DNA vectors. *Nat. Protoc.* **6,** 78–88 (2010).
28. Cachat, E. *et al.* 2- and 3-Dimensional Synthetic Large-Scale De Novo Patterning By Mammalian Cells Through Phase Separation. *Sci. Rep.* **6,** 20664 (2016).
29. Chen, A. Y., Zhong, C. & Lu, T. K. Engineering Living Functional Materials. *ACS Synth. Biol.* **4,** 8–11 (2015).
30. Zhou, D. *et al.* Highly branched poly(β-amino ester)s for skin gene therapy. *J. Control. Release* (2016). doi:10.1016/j.jconrel.2016.06.014
31. Cutlar, L. *et al.* A Non-Viral Gene Therapy for Treatment of Recessive Dystrophic Epidermolysis Bullosa. *Exp. Dermatol.* 818–820 (2016).
32. Deltcheva, E. *et al.* CRISPR RNA maturation by trans-encoded small RNA and host factor RNase III. *Nature* **471,** 602–609 (2011).
33. Jinek, M. *et al.* A Programmable Dual-RNA–Guided DNA Endonuclease in Adaptive Bacterial Immunity. *Science (80-.).* **337,** 816–821 (2012).
34. Fonfara, I., Richter, H., Bratovič, M., Le Rhun, A. & Charpentier, E. The CRISPR-associated DNA-cleaving enzyme Cpf1 also processes precursor CRISPR RNA CRISPR–Cas systems that provide defence against mobile genetic elements in bacteria and archaea have evolved a variety of mechanisms to target and cleave RNA or DNA. *Nature* **532,** 517–523 (2016).
35. Kay, M. A., He, C.-Y. & Chen, Z.-Y. A robust system for production of minicircle DNA vectors. *Nat. Biotechnol.* **28,** 1287–1289 (2010).
36. Yi, H. *et al.* A New Strategy to Deliver Synthetic Protein Drugs: Self-reproducible Biologics Using Minicircles. *Sci. Rep.* **4,** 5961 (2014).
37. Munye, M. M. *et al.* Minicircle DNA Provides Enhanced and Prolonged Transgene Expression Following Airway Gene Transfer. *Sci. Rep.* **6,** 23125 (2016).
38. Sibbald, B. Death but one unintended consequence of gene-therapy trial. *CMAJ* **164,** 1612 (2001).
39. Romero, Z., Toscano, M., Unciti, J., Molina, I. & Martin, F. Safer Vectors for Gene Therapy of Primary Immunodeficiencies. *Curr. Gene Ther.* **9,** 291–305 (2009).
40. Pisetsky, D. S. The origin and properties of extracellular DNA: from PAMP to DAMP. *Clin. Immunol.* **144,** 32–40 (2012).

41. Hotaling, N. a., Bharti, K., Kriel, H. & Simon, C. G. DiameterJ: A validated open source nanofiber diameter measurement tool. *Biomaterials* **61,** 327–338 (2015).

42. Lakes, R. Foam Structures with a Negative Poisson's Ratio. *Science (New York, N.Y.)* **235,** 1038–1040 (1987).

43. Greaves, G. N., Greer, A. L., Lakes, R. S. & Rouxel, T. Poisson's ratio and modern materials. *Nat. Mater.* **10,** 823–37 (2011).

44. Oliver, W. C. & Pharr, G. M. An improved technique for determining hardness and elastic modulus using load and displacement sensing indentation experiments. *Journal of Materials Research* **7,** 1564–1583 (2011).

45. Akhtar, R. *et al.* Nanoindentation of histological specimens: Mapping the elastic properties of soft tissues. *J. Mater. Res.* **24,** 638–646 (2009).

46. Livak, K. J. & Schmittgen, T. D. Analysis of relative gene expression data using real-time quantitative PCR and the 2-ÄÄCT method. *Methods* **25,** 402–408 (2001).

47. Callanan, A., Davis, N. F., McGloughlin, T. M. & Walsh, M. T. Development of a rotational cell-seeding system for tubularized extracellular matrix (ECM) scaffolds in vascular surgery. *J. Biomed. Mater. Res. Part B Appl. Biomater.* **102,** 781–788 (2014).

48. Bartlett, M. S. Properties of Sufficiency and Statistical Tests. *Proc. R. Soc. A Math. Phys. Eng. Sci.* **160,** 268–282 (1937).

49. Meier, U. A note on the power of Fisher's least significant difference procedure. *Pharm. Stat.* **5,** 253–263 (2006).

50. McHugh, M. L. Multiple comparison analysis testing in ANOVA. *Biochem. Medica* 203–209 (2011). doi:10.11613/BM.2011.029

51. Klaas, M. *et al.* The alterations in the extracellular matrix composition guide the repair of damaged liver tissue. *Sci. Rep.* **6,** 27398 (2016).

52. Kubow, K. E. *et al.* Mechanical forces regulate the interactions of fibronectin and collagen I in extracellular matrix. *Nat. Commun.* **6,** 8026 (2015).

53. Sottile, J. & Hocking, D. C. Fibronectin Polymerization Regulates the Composition and Stability of Extracellular Matrix Fibrils and Cell-Matrix Adhesions. *Mol. Biol. Cell* **14,** 3546–3559 (2002).

54. Discher, D. E., Janmey, P. & Wang, Y.-L. Tissue cells feel and respond to the stiffness of their substrate. *Science* **310,** 1139–43 (2005).

55. Klatt, D. *et al.* Viscoelastic properties of liver measured by oscillatory rheometry and multifrequency magnetic resonance elastography. *Biorheology* **47,** 133–141 (2010).

56. Torok, E. *et al.* Primary Human Hepatocytes on Biodegradable Poly(l-Lactic acid) Matrices: A Promising Model for Improving Transplantation Efficiency With Tissue Engineering. *Liver Transplant.* **13,** 465–466 (2011).

57. Loneker, A. E., Faulk, D. M., Hussey, G. S., D'Amore, A. & Badylak, S. F. Solubilized liver extracellular matrix maintains primary rat hepatocyte phenotype in-vitro. *J. Biomed. Mater. Res. A* 1–9 (2015).

58. Gao, R. *et al.* Hepatocyte Culture in Autologous Decellularized Spleen Matrix. *Organogenesis* (2015).

59. Martinez-Hernandez, A. & Amenta, P. S. The hepatic extracellular matrix I. Components and distribution in normal liver. *Virchows Arch. A Pathol. Anat.*

Histopathol. **423,** 1–11 (1993).

60. Cameron, K. *et al.* Recombinant Laminins Drive the Differentiation and Self-Organization of hESC-Derived Hepatocytes. *Stem Cell Reports* **5,** 1–13 (2015).

61. Pankov, R. & Yamada, K. M. Fibronectin at a glance. *J. Cell Sci.* **115,** 3861–3863 (2002).

62. Seliskar, M. & Rozman, D. Mammalian cytochromes P450-Importance of tissue specificity. *Biochim. Biophys. Acta - Gen. Subj.* **1770,** 458–466 (2007).

63. Medine, C. N. *et al.* Developing high-fidelity hepatotoxicity models from pluripotent stem cells. *Stem Cells Transl. Med.* **2,** 505–9 (2013).

64. Palakkan, A. A. *et al.* Polarisation and functional characterisation of hepatocytes derived from human embryonic and mesenchymal stem cells. *Biomed. reports* **3,** 626–636 (2015).

65. Saad, B. *et al.* Crude liver membrane fractions and extracellular matrix components as substrata regulate differentially the preservation and inducibility of cytochrome P-450 isoenzymes in cultured rat hepatocytes. *Eur J Biochem* **213,** 805–814 (1993).

66. Badylak, S. F. The extracellular matrix as a scaffold for tissue reconstruction. *Semin. Cell Dev. Biol.* **13,** 377–383 (2002).

67. Badylak, S. F., Dziki, J. L., Sicari, B. M., Ambrosio, F. & Boninger, M. L. Mechanisms by which acellular biologic scaffolds promote functional skeletal muscle restoration. *Biomaterials* **103,** 128–136 (2016).

68. Meng, F. W., Slivka, P. F., Dearth, C. L. & Badylak, S. F. Solubilized extracellular matrix from brain and urinary bladder elicits distinct functional and phenotypic responses in macrophages. *Biomaterials* **46,** 131–40 (2015).

69. Davis, N. F., Coakley, D. N., Callanan, A., Flood, H. D. & McGloughlin, T. M. Evaluation of xenogenic extracellular matrices as adjuvant scaffolds for the treatment of stress urinary incontinence. *Int. Urogynecol. J.* **24,** 2105–10 (2013).

70. He, M., Callanan, A., Lagaras, K., Steele, J. A. M. & Stevens, M. M. Optimization of SDS exposure on preservation of ECM characteristics in whole organ decellularization of rat kidneys. *J. Biomed. Mater. Res. Part B Appl. Biomater.* 1–9 (2016).

71. Burton, T. P., Corcoran, A. & Callanan, A. The effect of electrospun polycaprolactone scaffold morphology on human kidney epithelial cells. *Biomed. Mater* **13,** (2018).

72. Burton, T. P., Corcoran, A. & Callanan, A. The effect of electrospun polycaprolactone scaffold morphology on human kidney epithelial cells. *Biomed. Mater.* **13,** 15006 (2017).

73. Casasola, R., Thomas, N. L., Trybala, A. & Georgiadou, S. Electrospun poly lactic acid (PLA) fibres: Effect of different solvent systems on fibre morphology and diameter. *Polym. (United Kingdom)* **55,** 4728–4737 (2014).

74. Rafael Auras, Lim, L.-T., Selke, S. E. M. & Tsuji, H. *Poly(Lactic Acid): Synthesis, Structures, Properties, Processing, and Applications*. (2010).

75. Iwasaki, A. *et al.* Molecular mechanism responsible for fibronectin-controlled alterations in matrix stiffness in advanced chronic liver fibrogenesis. *J. Biol. Chem.* **291,** 72–88 (2016).

76. Zollinger, A. J. & Smith, M. L. Fibronectin, the extracellular glue. *Matrix Biol.* (2016).

doi:10.1016/j.matbio.2016.07.011

77. Kawelke, N. *et al.* Fibronectin protects from excessive liver fibrosis by modulating the availability of and responsiveness of stellate cells to active TGF-β. *PLoS One* **6,** e28181 (2011).

78. Altrock, E. *et al.* Inhibition of fibronectin deposition improves experimental liver fibrosis. *J. Hepatol.* **62,** 625–633 (2015).

79. George, E. L., Georges-Labouesse, E. N., Patel-King, R. S., Rayburn, H. & Hynes, R. O. Defects in mesoderm, neural tube and vascular development in mouse embryos lacking fibronectin. *Development* **119,** 1079–1091 (1993).

80. Costantini, S., Di Bernardo, G., Cammarota, M., Castello, G. & Colonna, G. Gene expression signature of human HepG2 cell line. *Gene* **518,** 335–45 (2013).

81. Gorell, E., Nguyen, N., Lane, A. & Siprashvili, Z. Gene therapy for skin diseases. *Cold Spring Harb Perspect Med* **4,** a015149 (2014).

82. Peloso, A. *et al.* Current achievements and future perspectives in whole-organ bioengineering. *Stem Cell Res. Ther.* **6,** (2015).

83. Woods, T. & Gratzer, P. F. Effectiveness of three extraction techniques in the development of a decellularized bone-anterior cruciate ligament-bone graft. *Biomaterials* **26,** 7339–7349 (2005).

84. Funamoto, S. *et al.* The use of high-hydrostatic pressure treatment to decellularize blood vessels. *Biomaterials* **31,** 3590–3595 (2010).

85. Cebotari, S. *et al.* Detergent decellularization of heart valves for tissue engineering: Toxicological effects of residual detergents on human endothelial cells. *Artif. Organs* **34,** 206–210 (2010).